ACS APPLIED MATERIALS & INTERFACES

Research Article

www.acsami.org

# Solventless Fabrication of Porous-on-Porous Materials

Philip Kwong,[†] Scott Seidel,[†] and Malancha Gupta*

Mork Family Department of Chemical Engineering and Materials Science, University of Southern California, 925 Bloom Walk, Los Angeles, California 90089, United States

**ABSTRACT:** Here we fabricate patterned porous polymer membranes on porous substrates by a combination of physical masking and chemical vapor deposition. This all-dry technique eliminates solvent-related issues and allows for the fabrication of hierarchical porous-on-porous structures with a wide range of chemical compositions and shapes. The porous polymer membranes are made by operating at unconventional processing conditions to simultaneously deposit and polymerize monomer. The solid monomer serves as a porogen and creates microstructures around which polymer forms. Membranes with thicknesses ranging from a few hundred micrometers to a millimeter are fabricated on porous paper substrates. The resolution of the patterning process and the structure of the resulting membranes are analyzed as a function of the deposition time. It was found that the patterned membranes exhibit a tapered structure and the dimensions are in good agreement with the dimensions of the mask. One potential application of these patterned polymer membranes is demonstrated for the selective separation of analytes for diagnostic applications on paper-based microfluidic devices. The ability to pattern porous-on-porous structures can be useful for the development of hierarchical membranes for water purification and gas separation, and for sensing, patterned tissue scaffolding, and other lab-on-a-chip applications.

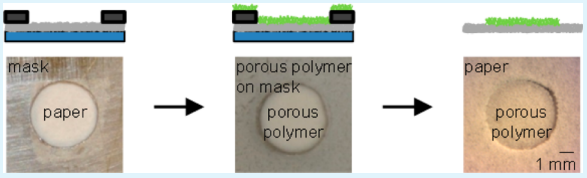


**KEYWORDS:** *polymer, porous polymer, membranes, chemical vapor deposition, functional polymers*

## INTRODUCTION

The fabrication of thin nonporous functional polymer films has led to significant advances for a wide range of applications including small-molecule detection[1] and biomolecule immobilization[2] and for dielectric[3] and hydrophobic[4] materials. However, the low surface area of these films can restrict their performance and limit their efficacy in certain applications.[5,6] To overcome this obstacle, porous polymer films can be used to vastly increase the surface area of the polymer to improve its usefulness, for example, for improved resolution in chemical[5] and biological[6,7] sensing applications. Furthermore, the added porosity and roughness can increase the potential utility of functional polymers to include uses as catalytic supports,[8] microreactors,[9] tissue scaffolds,[10−12] self-cleaning coatings,[13,14] and membranes.[15,16] The extension of porous polymers onto porous substrates allows for additional applications such as water purification. For example, Cadotte et al. fabricated porous polymer films on porous supports for reverse osmosis membranes,[17] and similar materials have recently been used in forward osmosis applications.[18]

Common methods for producing porous polymer films and membranes, including non-solvent induced phase separation,[19−21] thermally induced phase separation,[22−24] and the breath figure technique,[25−27] require the use of solvents, which may damage sensitive substrates or cause surface tension issues. Furthermore, the need to meet solubility requirements can limit both the chemical composition and morphology of the polymer structures attainable by these techniques. Vapor-phase polymer processing, which has conventionally been used to deposit thin conformal nonporous films,[1,3,28] has also recently been used to fabricate porous polymer films and membranes.[29−31] In these vapor-phase systems, the lack of solvents grants greater control over the polymer composition and substrate compatibility. In our recent work,[31] we described the ability to fabricate porous polymer membranes on planar surfaces using the initiated chemical vapor deposition (iCVD) process, which is a polymer processing technique typically used to generate nonporous films via adsorption and reaction of gaseous initiator and monomer molecules.[1,3,4] The porous polymer membranes were made by operating at unconventional iCVD processing conditions. The monomer partial pressures were increased above the saturation pressure and the substrate temperatures were kept below the freezing point of the monomer in order to simultaneously deposit and polymerize monomer. The frozen monomer served as a porogen and created pillar-like microstructures around which polymer formed. These pillar-like microstructures were believed to be caused by the use of operating conditions far from equilibrium, which resulted in the unstable growth of frozen monomer.[32] Following deposition, the solid monomer was removed, which resulted in membranes that contained two distinct pore sizes: large-scale pores on the order of tens of micrometers in diameter, which were formed during deposition by the void spaces between individual microstructures, and small-scale pores within the microstructures on the order of hundreds of nanometers in diameter, which were formed by the sublimation of the unreacted frozen monomer.

**Received:** July 11, 2013
**Accepted:** September 16, 2013
**Published:** September 27, 2013

   dx.doi.org/10.1021/am402775r | *ACS Appl. Mater. Interfaces* 2013, 5, 9714−9718

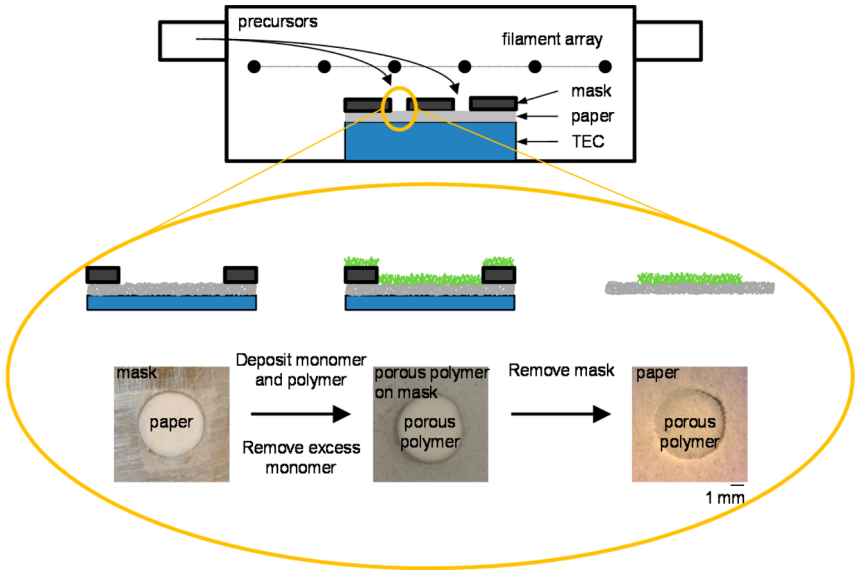


**Figure 1.** Schematic representation and optical images of the fabrication of patterned porous-on-porous materials.

In this paper, we demonstrate for the first time the solventless deposition of porous polymer membranes onto porous substrates allowing for the fabrication of hierarchical porous-on-porous materials, which could be used for water-purification and gas-separation applications.[17,33,34] Additionally, we demonstrate the ability to controllably pattern these porous-on-porous structures, which could further expand their utility to include sensing,[5−7] patterned tissue scaffolding,[10−12] and lab-on-a-chip applications.[1,35,36] By combining physical masking and chemical vapor deposition, our technique eliminates the use of solvents and thus can be generally applied to fabricate polymer membranes of varying chemical composition and shape on a wide variety of substrates. Membranes with thicknesses ranging from a few hundred micrometers to a millimeter composed of poly(methacrylic acid) (PMAA), a pH-responsive polymer that can enhance separations based on electrostatic interactions,[37,38] were patterned directly onto chromatography paper. The resolution of the patterning process and the structure of the resulting membranes were analyzed as a function of the deposition time. One potential application of these patterned polymer membranes was demonstrated for the selective separation of analytes on paper-based microfluidic devices.

## EXPERIMENTAL SECTION

Methacrylic acid (MAA; Aldrich, 99%), ethylene glycol diacrylate (EGDA; Aldrich, 90%), *tert*-butyl peroxide (Aldrich, 98%), chromatography paper (Whatman, No. 1), toluidine blue O (Aldrich, 80%), crystal violet (Aldrich, 90%), ponceau S (Aldrich, 75%), pH 6 buffer (BDH, ACS grade), and pH 8 buffer (BDH, ACS grade) were used as received without further purification.

Chromatography paper was placed on top of a thermoelectric cooler (TEC; TE Technology), which was located inside a pancake-shaped (250 mm diameter and 48 mm height) iCVD vacuum chamber (GVD Corp.).[39] Pressure was achieved by a rotary vane vacuum pump (Edwards E2M40) and maintained by a throttle valve (MKS 153D). A stainless steel mask with circular holes (2.7 mm radius) was placed on top of the chromatography paper with thermal grease (TE Technology) surrounding the outer edge of the mask. The substrate temperature was measured directly on top of the thermoelectric cooler with a thermocouple connected by thermal grease.

The initiator, *tert*-butyl peroxide, was kept at room temperature and introduced into the reactor at a flow rate of 0.7 sccm through a mass flow controller (MKS 1479A) to achieve a total pressure of 315 mTorr. A nichrome filament array (Omega Engineering, 80%/20% Ni/Cr) was subsequently heated to 250 °C to cleave the initiator into free radicals, and the thermoelectric cooler was equilibrated at −10 °C using an adjustable direct-current power supply (Volteq HY3010D). Finally, the monomer precursors were introduced; for the production of porous PMAA membranes, MAA was introduced at a flow rate of 4.0 sccm, and for the production of porous *x*PMAA membranes, MAA and EGDA were simultaneously introduced at flow rates of 4.0 and 0.1 sccm, respectively. The deposition times were varied between 2 and 30 min. Following deposition, all precursor flows were halted, the filament array was turned off, and the unreacted frozen monomer was sublimed at a thermoelectric cooler temperature of approximately 0 °C until the system returned to base pressure.

The structure of the samples was analyzed using a scanning electron microscope (JEOL-7001) at a 10 kV accelerating voltage. Gold was sputtered onto the samples for 30 s prior to imaging. Cross sections were observed by cutting the samples with scissors. The porous polymer membrane thickness and radius and the diameters of the large-scale pores were estimated from scanning electron micrographs and averaged over three separate depositions, with errors representing 1 standard deviation. The diameters of the large-scale pores were estimated from an area of approximately 1 $mm^2$ from top-down scanning electron micrographs of the interior of the membranes and processed as recommended by NIST using *ImageJ* (version 1.44p)[40] under the assumption of circular pores.

Dyeing of the porous *x*PMAA membranes was performed by immersing the samples in 0.001 wt % toluidine blue O in a buffered pH 8 solution for 12 h. The membranes were then washed three times by immersion in a buffered pH 8 solution for a total of 36 h. The membranes were then allowed to dry in ambient conditions and scanned using a color desktop printer (HP Deskjet F4480). The images were converted to gray scale, and line intensities were gathered using *ImageJ*. The intensities were normalized against unmodified chromatography paper treated with toluidine blue O in the same manner as that described above and averaged over two samples with two scans per sample taken perpendicular to each other.

Paper-based microfluidic devices were fabricated by printing wax (Xerox Phaser 8560N) onto Whatman chromatography paper and subsequently heating the paper to 180 °C for 3 min to melt the wax through the depth of the paper.[41,42] The ability of porous *x*PMAA membranes to selectively separate cationic analytes was analyzed by depositing porous *x*PMAA membranes for 10 min at the inlet of

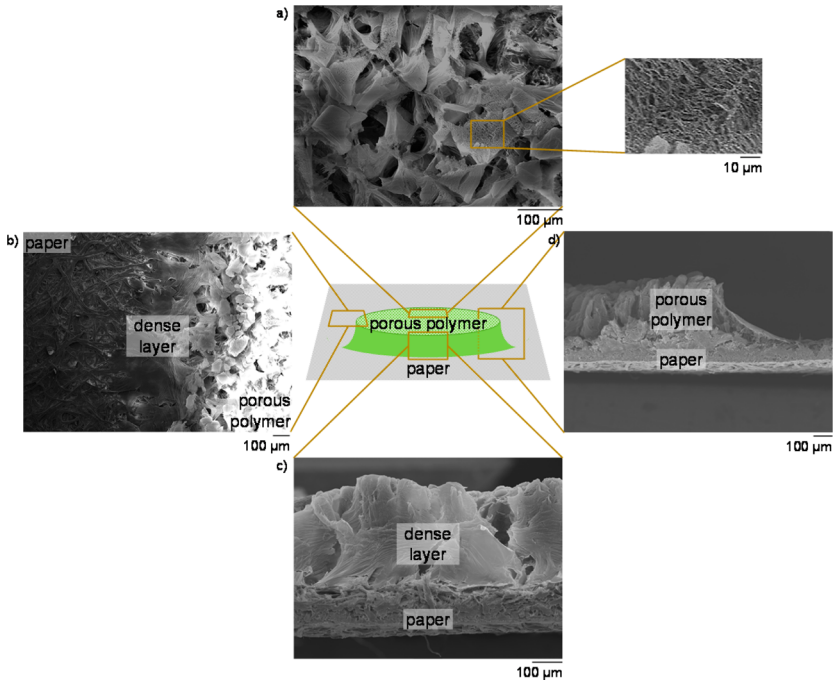


**Figure 2.** Schematic of the membrane structure with scanning electron micrographs showing the (a) top-down membrane morphology with an inset at higher magnification, (b) tapered edge, (c) exterior cross section, and (d) interior cross section.

paper-based microfluidic channels using a stainless steel mask, as described above. Three $\mu$L of a buffered pH 6 solution containing 2 mg/mL crystal violet and 0.25 mg/mL ponceau S was then applied to the inlet of the channel and allowed to flow through the device in ambient conditions. Separation of the dyes was performed using three separate channels to confirm the result.

## RESULTS AND DISCUSSION

In order to fabricate the patterned polymer membranes, a thermoelectric cooler was placed inside an iCVD vacuum chamber to achieve cold substrate temperatures (−10 °C) in order to satisfy the two requirements previously discussed:[31] the partial pressure of the monomer must be greater than its saturation pressure, and the temperature of the substrate must be less than the freezing point of the monomer (MAA; 14 °C). Chromatography paper was used as a porous substrate. The paper was placed on top of the thermoelectric cooler and covered with a stainless steel mask in order to pattern deposition of the polymer, as shown in Figure 1. During deposition, polymer visibly grew on both the mask and exposed paper. Following deposition, the unreacted frozen monomer was sublimed until the system returned to base pressure, leaving behind porous polymer membranes patterned directly onto the chromatography paper. While circular membranes were fabricated for demonstration, this technique can be extended to other shapes by simply varying the mask.

We examined the structure of the polymer membranes at deposition times of 10, 20, and 30 min using scanning electron microscopy (SEM). Lower deposition times (< 2 min) did not result in a cohesive polymer layer. For deposition times in the range of 10−30 min, the membrane thickness had a linear growth rate of 32.2 ± 2.8 $\mu$m/min. The radii of the base (polymer−paper interface) of the membranes (2.8 ± 0.1 mm) were in relatively good agreement with the radius of the mask (2.7 mm) for all deposition times, confirming successful patterning of the membranes. The radii of the top (polymer−air interface) of the membranes (2.3 ± 0.1 mm) were slightly smaller than the radius of the mask. The tapered structure of the membranes is attributed to shadowing effects during deposition caused by the mask and growing polymer, which has been similarly observed in other vapor-phase deposition systems including the oblique angle deposition of parylene[43] and the sputtering of metals,[44] leading to nonuniform deposition onto the substrate.

Morphologically, the interior of the membranes were composed of randomly aligned pillar-like microstructures and displayed dual-scale porosity similar to that of the membranes deposited onto planar substrates with large-scale pores on the order of tens of micrometers in diameter and small-scale pores on the order of hundreds of nanometers in diameter (Figure 2a).[31] The tapered edges (Figure 2b,c) of the membranes displayed a dense polymer layer that partially bridged individual microstructures. The interior cross-sectional image (Figure 2d) showed that this dense layer was restricted to the edge of the membranes while the interior remained highly porous. This dense layer likely forms as a result of the shadowing effects at the interface between the mask and growing polymer, which prevents deposition of additional solid monomer and formation of microstructures but still allows adsorbed monomer vapor to polymerize across the surface. Relative to deposition of membranes onto flat surfaces,[31] deposition onto porous substrates was more disordered, leading to a broad size distribution of the large-scale pores (Figure 3). The distribution of the pore diameters was independent of the deposition time, and membrane fabrication was reproducible with consistent morphology and an average pore diameter of approximately 30 ± 4 $\mu$m.

While the SEM images showed no polymer deposition outside the patterned area, we dyed cross-linked PMAA membranes with toluidine blue O[45] to further study whether the regions of chromatography paper covered by the mask were coated with polymer. The polymer was cross-linked to prevent dissolution during dyeing. In order to fabricate the cross-linked

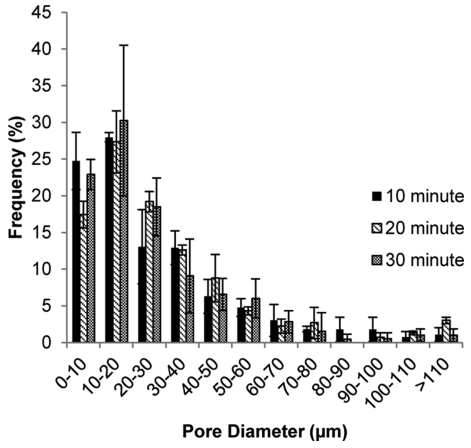


**Figure 3.** Distribution of the diameters of the large-scale pores for membranes fabricated at deposition times of 10, 20, and 30 min.

poly(MAA-*co*-EGDA) (*x*PMAA) membranes, EGDA was added into the reactor at a partial pressure below its saturation pressure to ensure that it did not affect the morphology of the porous membranes (Figure 4a). The *x*PMAA membranes were

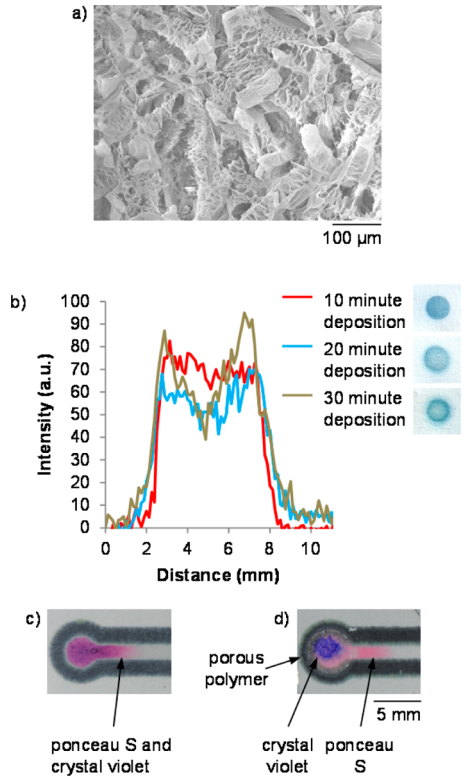


**Figure 4.** (a) Top-down scanning electron micrograph of a porous *x*PMAA membrane. (b) Intensity plot of dyed *x*PMAA membranes. Mixture of crystal violet and ponceau S flowing through a paper-based microfluidic device in the (c) absence and (d) presence of a porous *x*PMAA membrane.

fabricated at deposition times of 10, 20, and 30 min and analyzed to determine the locations of polymer deposition. The intensity plots of the polymer membranes (Figure 4b) show a radius and tapered edge, which is consistent with the structure of the membranes, as observed by SEM. Outside the area of the polymer membrane, the intensity quickly returns to the baseline for all deposition times, indicating that there is negligible deposition of polymer in the areas covered by the mask. The absence of polymer under the mask is attributed to the depletion of monomer from the vapor-phase as a result of its deposition, preventing diffusion of monomer vapor throughout the paper substrate. The absence of polymer allows our fabrication technique to be used in applications where patterning of polymer deposition is essential, such as in sensing and lab-on-a-chip applications.

As an example of the utility of these patterned porous-on-porous materials, we demonstrated their use as filters for paper-based microfluidic devices. Paper-based microfluidic devices are a new type of point-of-care devices,[46,47] but they generally lack the functionality available to pressure-driven microfluidic devices.[38,48] For instance, the ability of unmodified chromatography paper to separate analytes is limited, as shown by its inability to separate a mixture of crystal violet and ponceau S (Figure 4c). However, incorporation of a *x*PMAA porous polymer membrane patterned onto the inlet of a paper-based microfluidic device allows for selective separation of crystal violet as a model cationic analyte from a mixture containing the anionic dye ponceau S (Figure 4d). This separation is due to the increased electrostatic attraction between the electronegative *x*PMAA and the electropositive crystal violet, which is further enhanced by the high surface area provided by the porous polymer membrane.

## CONCLUSION

In summary, we have demonstrated the ability to fabricate patterned porous polymer membranes on porous substrates using a combination of physical masking and vapor-phase processing. In order to generate the porous morphology, deposition conditions were selected to simultaneously deposit and polymerize monomer. Our technique eliminates the use of solvents and allows for the fabrication of hierarchical porous-on-porous materials. The patterned membranes exhibited a tapered structure, and the dimensions were in good agreement with the dimensions of the mask. While the fabrication of circular PMAA and *x*PMAA membranes on chromatography paper was demonstrated, our technique can be easily expanded for the fabrication of porous polymers membranes of varying chemical composition and shape on a variety of porous substrates. The utility of these types of patterned porous-on-porous materials was shown for the selective separation of analytes for paper-based microfluidic applications, but their use can be extended for the development of hierarchical membranes for water purification and gas separation and for sensing, patterned tissue scaffolding, and other lab-on-a-chip applications.

## AUTHOR INFORMATION

### Corresponding Author

*E-mail: malanchg@usc.edu.

### Author Contributions

†These authors contributed equally.

### Notes

The authors declare no competing financial interest.

## ACKNOWLEDGMENTS

This work was supported by the National Science Foundation CAREER Award CMMI-1252651, the Alfred Mann Institute at the University of Southern California (P.K.), the Natural

Sciences and Engineering Research Council of Canada (P.K.), and the National Science Foundation Graduate Research Fellowship under Grant DGE-0937362 (S.S.).

## REFERENCES

(1) Tenhaeff, W. E.; McIntosh, L. D.; Gleason, K. K. *Adv. Funct. Mater.* **2010**, *20*, 1144−1151.
(2) Hwang, I.-T.; Kuk, I.-S.; Jung, C.-H.; Choi, J.-H.; Nho, Y.-C.; Lee, Y.-M. *ACS Appl. Mater. Interfaces* **2011**, *3*, 2235−2239.
(3) Trujillo, N. J.; Wu, Q.; Gleason, K. K. *Adv. Funct. Mater.* **2010**, *20*, 607−616.
(4) Gupta, M.; Gleason, K. K. *Langmuir* **2006**, *22*, 10047−10052.
(5) Yang, J.-S.; Swager, T. M. *J. Am. Chem. Soc.* **1998**, *120*, 11864−11873.
(6) Shen, Y.; Liu, Y.; Zhu, G.; Fang, H.; Huang, Y.; Jiang, X.; Wang, Z. L. *Nanoscale* **2013**, *5*, 527−531.
(7) Dong, H.; Cao, X.; Li, C. M. *ACS Appl. Mater. Interfaces* **2009**, *1*, 1599−1606.
(8) Xie, S.; Svec, F.; Fréchet, J. M. J. *Biotechnol. Bioeng.* **1999**, *62*, 30−35.
(9) Gömann, A.; Deverell, J. A.; Munting, K. F.; Jones, R. C.; Rodemann, T.; Canty, A. J.; Smith, J. A.; Guijt, R. M. *Tetrahedron* **2009**, *65*, 1450−1454.
(10) Cameron, N. R. *Polymer* **2005**, *46*, 1439−1449.
(11) Beattie, D.; Wong, K. H.; Williams, C.; Poole-Warren, L. A.; Davis, T. P.; Barner-Kowollik, C.; Stenzel, M. H. *Biomacromolecules* **2006**, *7*, 1072−1082.
(12) Mattanavee, W.; Suwantong, O.; Puthong, S.; Bunaprasert, T.; Hoven, V. P.; Supaphol, P. *ACS Appl. Mater. Interfaces* **2009**, *1*, 1076−1085.
(13) Levkin, P. A.; Svec, F.; Fréchet, J. M. J. *Adv. Funct. Mater.* **2009**, *19*, 1993−1998.
(14) Hwang, H. S.; Kim, N. H.; Lee, S. G.; Lee, D. Y.; Cho, K.; Park, I. *ACS Appl. Mater. Interfaces* **2011**, *3*, 2179−2183.
(15) Pinnau, I.; Koros, W. J. *J. Appl. Polym. Sci.* **1991**, *43*, 1491−1502.
(16) Nuxoll, E. E.; Hillmyer, M. A.; Wang, R.; Leighton, C.; Siegel, R. A. *ACS Appl. Mater. Interfaces* **2009**, *1*, 888−893.
(17) Cadotte, J. E.; Petersen, R. J.; Larson, R. E.; Erickson, E. E. *Desalination* **1980**, *32*, 25−31.
(18) McCutcheon, J. R.; McGinnis, R. L.; Elimelech, M. *Desalination* **2005**, *174*, 1−11.
(19) Loeb, S.; Sourirajan, S. In *Saline Water Conversion-II*; Gould, R. F., Ed.; ACS Advances in Chemistry Series; American Chemical Society: Washington, DC, 1963; Vol. *38*, pp 117−132.
(20) Reuvers, A. J.; Smolders, C. A. *J. Membr. Sci.* **1987**, *34*, 67−86.
(21) Rangarajan, R.; Desai, N. V.; Mody, R. C.; Mohan, D.; Rao, A. V. *Desalination* **1991**, *85*, 81−92.
(22) Caneba, G. T.; Soong, D. S. *Macromolecules* **1985**, *18*, 2538−2545.
(23) Lo, H.; Ponticiello, M. S.; Leong, K. W. *Tissue Eng.* **1995**, *1*, 15−28.
(24) Matsuyama, H.; Yuasa, M.; Kitamura, Y.; Teramoto, M.; Lloyd, D. R. *J. Membr. Sci.* **2000**, *179*, 91−100.
(25) Park, J. S.; Lee, S. H.; Han, T. H.; Kim, S. O. *Adv. Funct. Mater.* **2007**, *17*, 2315−2320.
(26) Cai, Y.; Newby, B.-M. Z. *Langmuir* **2009**, *25*, 7638−7645.
(27) Wu, X.; Wang, S. *ACS Appl. Mater. Interfaces* **2012**, *4*, 4966−4975.
(28) Seidel, S.; Riche, C.; Gupta, M. *Encycl. Polym. Sci. Technol.* **2011**, DOI: 10.1002/0471440264.pst467.
(29) Demirel, M. C.; So, E.; Ritty, T. M.; Naidu, S. H.; Lakhtakia, A. *J. Biomed. Mater. Res.* **2007**, *81B*, 219−223.
(30) Demirel, G.; Malvadkar, N.; Demirel, M. C. *Thin Solid Films* **2010**, *518*, 4252−4255.
(31) Seidel, S.; Kwong, P.; Gupta, M. *Macromolecules* **2013**, *46*, 2976−2983.
(32) Imai, H.; Oaki, Y.; Kotachi, A. *Bull. Chem. Soc. Jpn.* **2006**, *79*, 1834−1851.
(33) Kesting, R. E. *J. Appl. Polym. Sci.* **1990**, *41*, 2739−2752.
(34) Petersen, R. J. *J. Membr. Sci.* **1993**, *83*, 81−150.
(35) Simms, H. M.; Brotherton, C. M.; Good, B. T.; Davis, R. H.; Anseth, K. S.; Bowman, C. N. *Lab Chip* **2005**, *5*, 151−157.
(36) Mair, D. A.; Schwei, T. R.; Dinio, T. S.; Svec, F.; Fréchet, J. M. J. *Lab Chip* **2009**, *9*, 877−883.
(37) Boardman, N. K. *J. Chromatogr. A* **1959**, *2*, 388−397.
(38) Kwong, P.; Gupta, M. *Anal. Chem.* **2012**, *84*, 10129−10135.
(39) Kwong, P.; Flowers, C. A.; Gupta, M. *Langmuir* **2011**, *27*, 10634−10641.
(40) NIST Index of Image Processing Labs, http://www.nist.gov/lispix/imlab/ (accessed Sept 15, 2012).
(41) Lu, Y.; Shi, W.; Jiang, L.; Qin, J.; Lin, B. *Electrophoresis* **2009**, *30*, 1497−1500.
(42) Carrilho, E.; Martinez, A. W.; Whitesides, G. M. *Anal. Chem.* **2009**, *81*, 7091−7095.
(43) He, M.; Wang, P.-I.; Lu, T.-M. *Langmuir* **2011**, *27*, 5107−5111.
(44) Rossnagel, S. M.; Nichols, C.; Hamaguchi, S.; Ruzic, D.; Turkot, R. *J. Vac. Sci. Technol. B* **1996**, *14*, 1819−1827.
(45) Ma, Z.; Kotaki, M.; Ramakrishna, S. *J. Membr. Sci.* **2006**, *272*, 179−187.
(46) Martinez, A. W.; Phillips, S. T.; Butte, M. J.; Whitesides, G. M. *Angew. Chem., Int. Ed.* **2007**, *46*, 1318−1320.
(47) Yetisen, A. K.; Akram, M. S.; Lowe, C. R. *Lab Chip* **2013**, *13*, 2210−2251.
(48) Focke, M.; Kosse, D.; Müller, C.; Reinecke, H.; Zengerle, R.; von Stetten, F. *Lab Chip* **2010**, *10*, 1365−1386.